Korean J. Chem. Eng., **29**(3), 404-412 (2012)
DOI: 10.1007/s11814-011-0182-6

A crossover quasi-chemical nonrandom lattice fluid model for pure carbon dioxide and hydrocarbons

Moon Sam Shin*, Sujin Kim, and Hwayong Kim***,†**

*Department of Dermatological Health Management, Eulji University,
212, Yangji-dong, Sujeong-gu, Seongnam-si, Gyeonggi-do 461-713, Korea
**Department of Cosmetic Science, Chungwoon University, San 29, Namjang-ri, Hongseoung-gun, Chungnam 350-701, Korea
***School of Chemical & Biological Engineering, Seoul National University, Shinlim-dong, Gwanak-gu, Seoul 151-744, Korea
(*Received 14 February 2011 • accepted 17 July 2011*)

Abstract–Thequasi-chemical nonrandom lattice fluid model is capable of describing thermodynamic properties for complex systems containing associating fluids, polymer, biomolecules and surfactants, but this model fails to reproduce the singular behavior of fluids in the critical region. In this research, we used the quasi-chemical nonrandom lattice fluid model and combined this model with a crossover theory to obtain a crossover quasi-chemical nonrandom lattice fluid model which incorporated the critical scaling laws valid asymptotically close to the critical point and reduced to the original quasi-chemical nonrandom model far from the critical point. The crossover quasi-chemical nonrandom lattice fluid model showed a great improvement in prediction of the volumetric properties and second-order derivative properties near the critical region.

Key words: Crossover, Quasi-chemical, Lattice Model, Critical Region, Second-order, Derivative Properties

INTRODUCTION

Phase equilibrium properties and thermodynamic second-order derivative properties (e.g., heat capacities, isothermal compressibility, thermal expansion coefficient, the Joule-Thomson coefficient, and the sound speed) are required for design of separation operations and chemical plants over a wide range of temperature and pressure. Due to their central importance to the practice of chemical engineering, many thermodynamic models have been developed, based on theory and on empiricism. Whenapplied in normal conditions far from the critical regions, classical lattice models can accurately calculate and predict physical properties. However, the statistical mechanical theories point out that fluids have density fluctuations. Far from the critical point, the density fluctuations affect slightly the thermodynamic properties and would be neglected. Most thermodynamic models could use the mean-field theories [1] to represent properties of fluids far away from the critical point, so these models [2-6] fail to satisfactorily reproduce physical properties near the critical region. In a large compressibility region such as the critical region, the fluctuations of fluids becomevery large and some singular phenomena and properties, such as the critical emulsification phenomenon, take place. To improve the description of the gas-liquid critical locus for pure fluids, the lattice model parameters can be rescaled [7] to the experimental pure fluid critical point, and an accurate representation of the critical locus is obtained. However, despite the success achieved using rescaled lattice model, poor agreement is obtained at lower pressures, especially at lower temperatures and for the coexisting liquid densities. Several researches have been presented to overcome the deficiency of classical thermodynamic models in describing physical properties in the vicinity of a critical point during the past forty years. The most remarkable result of these studies has been the discovery of critical-point universality: The microscopic structure of fluids becomes unimportant near the critical point [8]. The discovery makes it possible to developuniversal equations of state for fluids in the critical region and enables us to look into the problem of formulating global equations of state for dense fluids from an entirely new point of view. Due to density fluctuations, some physicalproperties, such as the isothermal compressibility and the isochoric heat capacity, vary discontinuously near the critical region. From spectroscopic experimental data and molecular simulation, the limiting values of the differential molar volume, the differential molar enthalpy and the differential molar heat capacity in the region around the critical pointcould be related to the distance from the critical point. From the viewpoint of thedistance from the critical point, the scaling laws with universal scaling functions and universal critical exponents could markthe thermodynamic behaviors in the vicinity of a critical point [9]. Kiselev and coworkers presented a crossover cubic model [10] and crossover SAFT model [11] that provided successful representations of the thermodynamic and second order properties of fluids near to and far from the critical region.

In the former researches [12-15], the present authors presented a crossover cubic model and crossover Sanchez-Lacombe lattice fluid model that combinedthe crossover scale laws valid asymptotically close to the critical point and reduced to the original thermodynamic models far from the critical point. The Sanchez-Lacombe lattice fluid model used the full Guggenheim combinatory but had the assumptions that the nonrandom contribution was negligible and that this model took up the large coordination number limit known as the Flory approximation.

In this study, we chose the quasi-chemical nonrandom lattice fluid

†To whom correspondence should be addressed.
E-mail: hwayongk@snu.ac.kr

model as a reference model and combined it with the crossover theory to obtain a crossover quasi-chemical nonrandom lattice fluid model and to calculate the thermodynamic properties near to and far from the critical point. We also evaluated the crossover quasi-chemical nonrandom lattice fluid model to phase equilibria properties and second-order derivative properties for some pure systems over a wide range to include the critical region.

CROSSOVER QUASI-CHEMICAL NONRANDOM LATTICE FLUID MODEL

The lattice model (NLF) model [16,17] was developed on quasi-chemical approach of the lattice theory and extended to complex systems containing associating fluids [18] and polymers [19]. However, the NLF model has strong temperature dependence of energy parameters and segment numbers of pure systems thus empirical correlations as functions of temperature were adopted for reliable and convenient use in engineering practices. We recently presented a new version of the quasi-chemical nonrandom lattice fluid (QLF) model [4] with no temperature dependent molecular parameters and obtained the expression of fugacity coefficients for phase equilibrium calculations. This QLF model was capable of describing thermodynamic properties for complex systems containing associating fluids [20], surfactants [21,22], polymer [23] and biomolecules [24,25]. However, this classical QLF model is not applicable in the vicinity of a critical point due to mean-field approximation.

In this study, the QLF model with quasi-chemical approach was chosen as a reference lattice fluid model and was represented as follows:

$$\frac{\tilde{P}}{\tilde{T}} = -\ln(1-\tilde{\rho}) + \frac{z}{2}\ln\left[1+\left(\frac{q}{r}-1\right)\tilde{\rho}\right] - \frac{\theta^2}{\tilde{T}} \tag{1}$$

Here, all the quantities with the tilde (~) denote the reduced variables defined by

$$\tilde{P} = \frac{P}{P^*},\quad \tilde{T} = \frac{T}{T^*},\quad \tilde{\rho} = \frac{\rho}{\rho^*},\quad \rho^* = \frac{1}{rv^*} \tag{2}$$

where the reducing parameters are defined by

$$P^* v_1^* = kT^* = \frac{z}{2}\varepsilon_M \tag{3}$$

and ε_M is defined by

$$\varepsilon_M = \frac{1}{\theta^2}\left[\sum_{i=0}^{1}\sum_{j=0}^{1}\theta_i\theta_j\varepsilon_{ij} + \frac{\beta}{2}\sum_{i=0}^{1}\sum_{j=0}^{1}\sum_{k=0}^{1}\sum_{l=0}^{1}\theta_i\theta_j\theta_k\theta_l\varepsilon_{ij}(\varepsilon_{ij}+3\varepsilon_{kl}-2\varepsilon_{ik}-2\varepsilon_{jk})\right] \tag{4}$$

Here θ is the effective surface area fraction of molecules in the lattice,

$$\theta = \frac{N_1 q_1}{N_q} = \frac{(q/r)\tilde{\rho}}{1+(q/r-1)\tilde{\rho}} = 1-\theta_0 \tag{5}$$

Let us set coordination number, z=10 as used in lattice fluid theories of the same genre [26,27].

The QLF model has three molecular parameters; ε^*, v^*, and r, which are equivalently of the scale factors T^*, P^*, and ρ^*.

The residual Helmholtz free energy $A^r(T, v)$ was obtained as follows:

$$A^r(T,v) = -\int_{\infty}^{V}\left(P-\frac{nRT}{V}\right)dV = nrRT\left[\left(\frac{1}{\tilde{\rho}}-1\right)\ln(1-\tilde{\rho})\right] - RT\left[\frac{znr}{2}\tilde{\rho}+n(1-r)\right]\ln\left(1+\left(\frac{q}{r}-1\right)\tilde{\rho}\right)+nRT-\frac{nqRT\theta}{\tilde{T}} \tag{6}$$

The molar Helmholtz free energy can be written as

$$a(T,v) = a^r(T,v) + a^{id}(T,v) \tag{7}$$

where $a^r(T, v)$ is the residual molar Helmholtz free energy and $a^{id}(T, v)$ is the molar Helmholtz free energy for ideal gas

$$a^{id}(T,v) = -RT\ln v + a_0(T) \tag{8}$$

In Eq. (8), $a_0(T)$ is the temperature-dependent part of the Helmholtz free energy for ideal gas.

The classical expression for the Helmholtz free energy $\overline{A}(T, v)$ was rewritten in the dimensionless form as follows:

$$\overline{A}(T,v) = \frac{a(T,v)}{RT} = \overline{A}^r(T,v) - \ln v + \overline{A}_0(T) \tag{9}$$

$$\overline{A}^r(T,v) = r\left[\left(\frac{1}{\tilde{\rho}}-1\right)\ln(1-\tilde{\rho})\right] - \left[\frac{zr}{2}\tilde{\rho}+(1-r)\right]\ln\left(1+\left(\frac{q}{r}-1\right)\tilde{\rho}\right)+1-\frac{q\theta}{\tilde{T}} \tag{10}$$

The classical critical parameters T_{oc}, P_{oc} and v_{oc} of classical model

Table 1. Molecular parameters for the crossover quasi-chemical nonrandom lattice fluid (xQLF) EOS

Components	Classical parameters			Crossover parameters		
	T^*/K	P^*/MPa	ρ^*/g cm^{-3}	Gi	v_1	d_1
Carbon dioxide	272.83	1280.56	1.432	0.1154	0.0025	8.4895
Methane	265.13	80.63	0.243	0.2424	0.0005	−0.1195
Ethane	384.56	140.58	0.298	0.1742	0.0006	0.0128
Propane	462.38	159.64	0.425	0.1194	0.0008	0.0104
n-Butane	523.14	140.34	0.432	0.1406	0.0010	0.0095
n-Pentane	451.34	205.67	0.447	0.3394	0.0011	0.8527
n-Hexane	480.64	330.62	0.557	0.1238	0.0013	2.1056
n-Heptane	498.64	363.82	0.581	0.1242	0.0017	2.3484

Table 2. Kernel term parameters for the xQLF model

	Carbon dioxide	Methane	Ethane	Propane
a_{20}	14.558	10.138	12.986	13.087
a_{21}	−3.578	−1.348	−3.894	−2.538

can be obtained from the condition

$$\left(\frac{\partial P}{\partial \rho}\right)_{T_{oc}} = \left(\frac{\partial^2 P}{\partial \rho^2}\right)_{T_{oc}} = 0 \tag{11}$$

The Sanchez-Lacombe model has analytical expressions [2,3] for the classical critical properties, but the QLF model cannot obtain analytical expressions. Since it is hard to straightly obtain the classical critical properties for the QLF model, a method of getting them is required. Minimum of $\partial P/\partial \rho$, $(\partial P/\partial \rho)|_{min}$ is less than zero for $T<T_{oc}$ and $(\partial P/\partial \rho)|_{min}$ is greater than zero for $T>T_{oc}$. Therefore, $(\partial P/\partial \rho)|_{min}$ is zero at the classical critical temperature and volume:

$$\left.\frac{\partial P}{\partial \rho}\right|_{min} = 0 \text{ at } T = T_{oc},\ v = v_{oc} \tag{12}$$

$$P_{oc} = P^* \tilde{T}_{oc}\left[-\ln(1-\tilde{P}_{oc}) + \frac{z}{2}\ln\left[1+\left(\frac{q}{r}-1\right)\tilde{\rho}_{oc}\right] - \frac{\theta_{oc}}{\tilde{T}}\right] \tag{13}$$

where $\theta_{oc} = \dfrac{(q/r)\tilde{\rho}_{oc}}{1+(q/r-1)\tilde{\rho}_{oc}}$ (14)

To derive the crossover quasi-chemical nonrandom lattice fluid (xQLF) model, we need to recast the classical expression for Helmholtz free energy into dimensionless form as follows:

$$\overline{A}(T,v) = \Delta\overline{A}(\Delta T,\Delta v) + \overline{A}_{bg}(\Delta T,\Delta v) = \overline{A}^r(\Delta T,\Delta v) - \overline{A}^r(\Delta T,0) - \ln(\Delta v+1) + \Delta v\overline{P}_0(\Delta T) - \Delta v\overline{P}_0(T) + \overline{A}_0^r(T) + \overline{A}_0(T) - \ln v_{oc} \tag{15}$$

where $\Delta T = T/T_{oc} - 1$, $\Delta v = v/v_{oc} - 1$ are dimensionless distances from the classical temperature T_{oc} and molar volume v_{oc}, respectively. $\overline{P}_0(T) = P(T, v_{oc})/RT$ is the dimensionless pressure, $\overline{A}_0^r(T) = \overline{A}^r(T, v_{oc})$ is the dimensionless residual part of the Helmholtz free energy along the critical isochore $v = v_{oc}$. Then we replace the classical dimensional temperature ΔT and Δv in the critical term with renormalized values.

Table 4. The deviations of PρT properties with the QLF, the xQLF, the xLF and the xCubic model

Components	AADP[a]				T range/K
	QLF	xQLF	xLF	xCubic	
Carbon dioxide	13.24	0.76	1.07	1.92	260 to 340
Methane	32.54	0.92	1.84	1.38	150 to 230
Ethane	10.27	0.85	1.45	1.87	260 to 340
Propane	13.54	0.98	1.87	1.93	320 to 420
n-Butane	34.27	1.25	1.78	2.07	380 to 480
n-Pentane	24.63	0.86	1.34	1.75	440 to 540
n-Hexane	21.39	0.76	1.46	1.54	460 to 560
n-Heptane	19.37	0.91	1.46	1.61	480 to 580

[a] $AADP^{sat} = (1/n)\cdot\left(\sum_i^n \left|(P_{i,exp}^{Sat.} - P_{i,calc}^{Sat.})/P_{i,exp}^{Sat.}\right|\right)\times 100$

$$\overline{\tau} = \tau Y^{-\frac{\alpha}{2\Delta_1}} + (1+\tau)\Delta\tau_c Y^{\frac{2(2-\alpha)}{3\Delta_1}} \tag{16}$$

$$\overline{\varphi} = \varphi Y^{\frac{(\gamma-2\beta)}{4\Delta_1}} + (1+\varphi)\Delta v_c Y^{\frac{2(2-\alpha)}{2\Delta_1}} \tag{17}$$

where α=0.11, β=0.325, $\gamma = 2-2\beta-\alpha$=1.24 and Δ_1=0.51 are universal non-classical critical exponents [9]. $\tau = (T/T_c)-1$ is a dimensionless deviation of the temperature from the real critical temperature (T_c), $\varphi = (v/v_c)-1$ is a dimensionless deviation of the molar volume from the real critical molar volume (v_c), and $\Delta\tau_c = (T_c/T_{oc})-1$, $\Delta v_c = (v_c/v_{oc})-1$.

The crossover function Y can be written in the parametric form

$$Y(q) = \left(\frac{q}{1+q}\right)^{2\Delta_1} \tag{18}$$

where q is a renormalized distance to the critical point and can be found from the solution of the crossover sine-model (SM) [28].

$$\left(q^2 - \frac{\tau}{Gi}\right)\left[1 - \frac{p^2}{4b^2}\left(1 - \frac{\tau}{q^2 Gi}\right)\right] = b^2\left\{\frac{\varphi[1+v_1\exp(-10\varphi)] + d_1\tau}{m_0 Gi^{\beta}}\right\}^2 Y^{\frac{(1-2\beta)}{\Delta_1}} \tag{19}$$

where b^2 is the universal linear-model parameter and p^2 the univer-

Table 3. Calculated deviations of saturated properties with the QLF, the xQLF, the xLF and the xCubic model

Fluids	$AADP^{sat,a}$				$AAD\rho^b$				T range /K
	QLF	xQLF	xLF	xCubic	QLF	xQLF	xLF	xCubic	
Carbon dioxide	1.18	0.34	1.01	0.44	1.34	0.65	0.86	0.96	240 to 304
Methane	1.18	0.77	1.95	1.72	1.54	0.69	0.46	0.19	150to 190
Ethane	0.94	0.46	1.92	0.88	1.15	0.21	0.24	0.88	240 to 305
Propane	0.97	0.21	1.29	0.25	1.07	0.34	0.42	0.95	290 to 369
n-Butane	0.95	0.39	1.98	0.43	1.93	0.15	0.75	0.13	340 to 425
n-Pentane	1.04	0.21	0.71	0.16	1.26	0.48	0.60	1.12	400 to 469
n-Hexane	1.54	0.84	1.99	0.90	1.34	0.38	0.46	2.51	440 to 507
n-Heptane	1.59	0.75	1.91	0.66	1.58	0.43	0.46	1.15	480 to 540

[a] $AADP^{sat} = (1/n)\cdot\left(\sum_i^n \left|(P_{i,exp}^{Sat.} - P_{i,calc}^{Sat.})/P_{i,exp}^{Sat.}\right|\right)\times 100$

[b] $AAD\rho = (1/n)\cdot\left(\sum_i^n \left|(\rho_{i,exp}^{Sat.} - \rho_{i,calc}^{Sat.})/\rho_{i,exp}^{Sat.}\right|\right)\times 100$

sal sine-model parameters, $p^2=b^2=1.359$. Gi is the Ginzburg number for the fluid of interest [29] and we set $m_0=1$ in this study. Therefore, v_l, d_l, and Gi are the system-dependent parameters.

We added the Kernel term, $K(\tau, \varphi)$ to the Helmholtz expression, which provides the correct representation of the isochoric heat capacity asymptotically close to the critical point.

$$K(\tau,\varphi)=\frac{1}{2}a_{20}\tau^2[Y^{-\alpha/\Delta_1}(\tau,\varphi)-1]+\frac{1}{2}a_{21}\tau^2[Y^{-(\alpha-\Delta_1)/\Delta_1}(\tau,\varphi)-1] \quad (20)$$

where the coefficient a_{20} is the asymptotic term and a_{21} is the first Wegner-correction term.

The crossover form of the Helmholtz free energy can be written as

$$\overline{A}(T,v)=\Delta\overline{A}(\overline{\tau},\overline{\varphi})-\Delta v\overline{P}_0(T)+\overline{A}_0^r(T)+\overline{A}_0(T)-\ln v_{oc}-K(\tau,\varphi) \quad (21)$$

and the critical part, $\Delta\overline{A}$ is given by

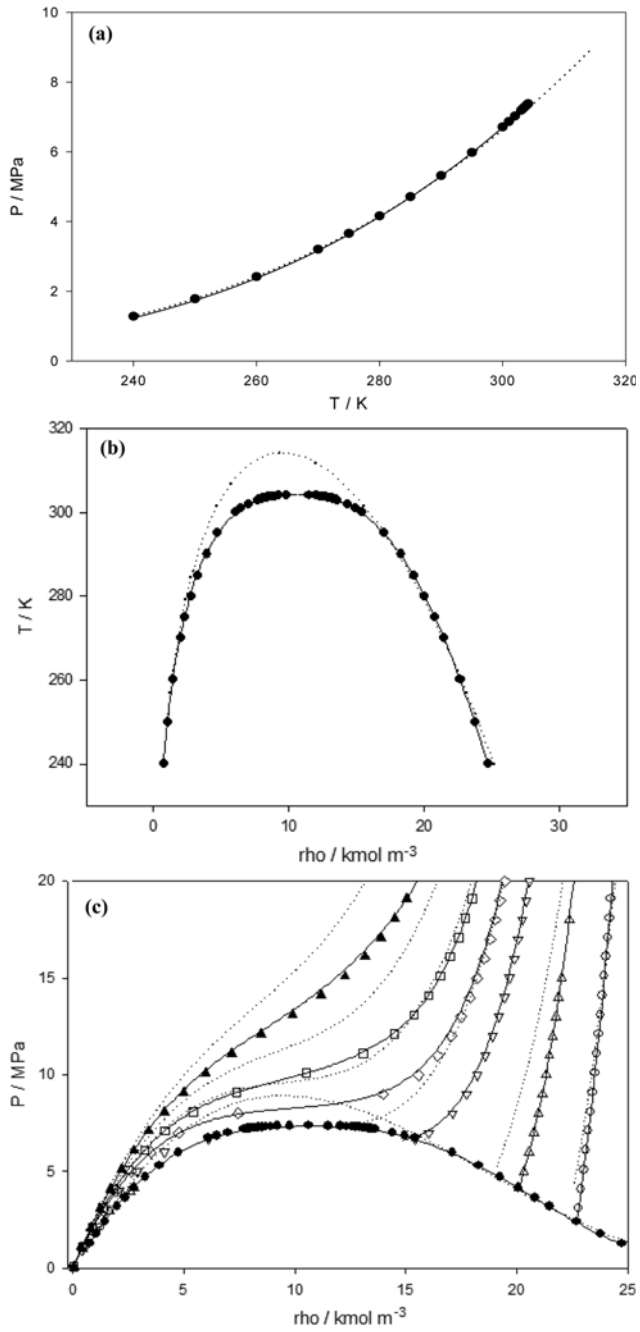

Fig. 1. Plot of thermodynamic properties with predictions of the QLF EOS (dotted curves), the xQLF EOS (solid curves) for carbon dioxide. (a) vapor pressure, (b) saturated density, (c) PρT: ●, saturated data; ○, 260 K; △, 280 K; ▽, 300 K; ◇, 310 K; □, 320 K; ▲, 340 K.

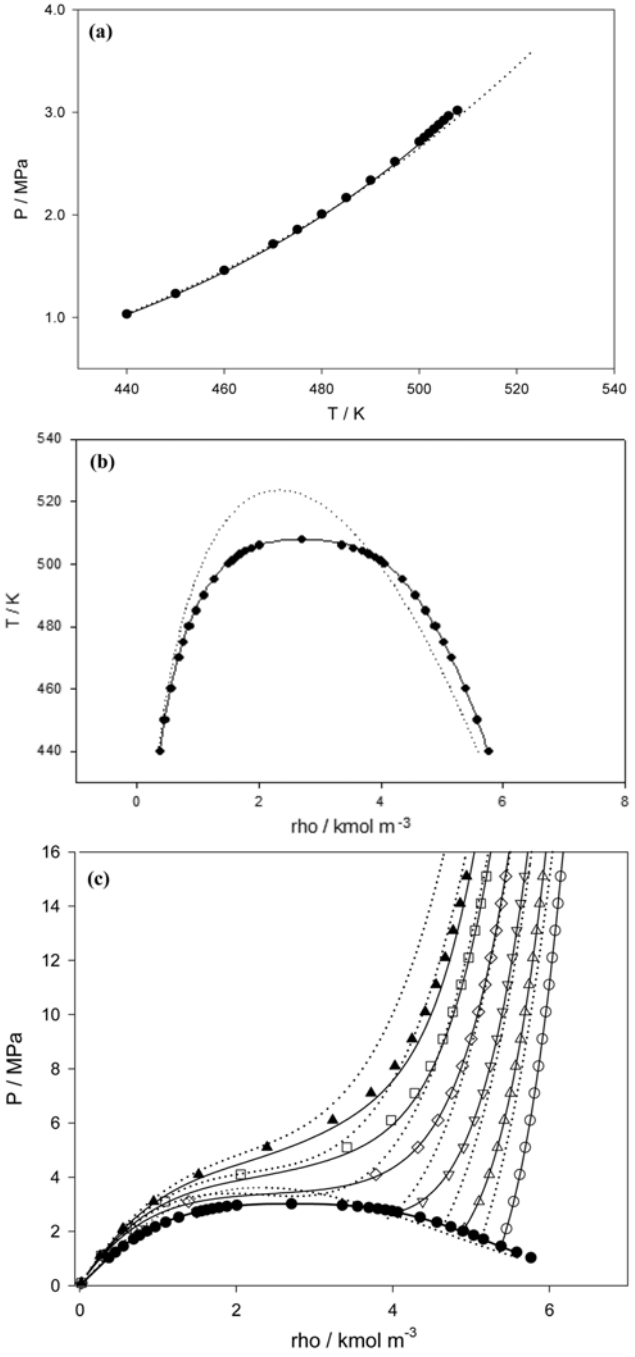

Fig. 2. Plot of thermodynamic properties with predictions of the QLF EOS (dotted curves), the xQLF EOS (solid curves) for n-hexane. (a) vapor pressure, (b) saturated density, (c) PρT: ●, saturated data; ○, 460 K; △, 480 K; ▽, 500 K; ◇, 520 K; □, 540 K; ▲, 560 K.

$$\Delta\bar{A}(\bar{\tau},\bar{\varphi}) = \bar{A}^{r}(\bar{\tau},\bar{\varphi}) - \bar{A}^{r}(\bar{\tau},0) - \ln(\bar{\varphi}+1) + \bar{\varphi}\bar{P}_0(\bar{\tau},0) \quad (22)$$

The xQLF model can be obtained by differentiation of Eq. (21) with respect to volumeas follows:

$$P(T,v) = -\left(\frac{\partial A}{\partial v}\right)_T = \frac{RT}{v_{oc}}\left[-\frac{v_{oc}}{v_c}\left(\frac{\partial \Delta\bar{A}(\bar{\tau},\bar{\varphi})}{\partial\varphi}\right)_T - \left(\frac{\partial K}{\partial\varphi}\right)_T + \bar{P}_0(T)\right] \quad (23)$$

Thermodynamic second derivative properties can be represented by derivatives of the Helmholtz energy and the pressure. Hence, the expressions for the derivative properties in this work are

$$C_v = -T\left(\frac{\partial^2 A}{\partial T^2}\right)_v = -T\left(\frac{\partial^2 A^{res}}{\partial T^2}\right)_v + C_c^{ideal} \quad (24)$$

$$\kappa_T = \frac{1}{\rho}\left(\frac{\partial P}{\partial\rho}\right)_T^{-1} \quad (25)$$

$$\alpha = \frac{1}{v}\left(\frac{\partial v}{\partial T}\right)_p = \kappa_T\left(\frac{\partial P}{\partial T}\right)_v \quad (26)$$

Table 5. Calculated deviations for thermodynamic second derivative properties

Compound	Property	P/MPa	AAD% QLF	AAD% xQLF	Compound	Property	P/MPa	AAD% QLF	AAD% xQLF
Carbon dioxide	C_p	7.377	14.7	5.07	Methane	C_p	4.599	11.5	6.05
		7.5	16.5	5.16			4.8	12.9	6.24
		8.0	18.7	6.54			5.1	13.6	8.01
		8.5	20.6	8.56			5.4	13.8	8.29
	κ_T	7.377	18.6	4.26		κ_T	4.599	20.1	3.01
		7.5	20.8	4.45			4.8	20.5	4.21
		8.0	25.6	6.23			5.1	21.6	6.06
		8.5	28.9	7.58			5.4	22.8	8.27
	α	7.377	27.5	4.01		α	4.599	20.6	3.13
		7.5	25.6	3.08			4.8	21.5	3.08
		8.0	30.6	5.64			5.1	22.6	4.16
		8.5	31.8	7.58			5.4	23.8	4.48
	μ	7.377	10.6	5.92		μ	4.599	13.8	4.42
		7.5	10.1	5.08			4.8	14.1	5.05
		8.0	11.6	5.15			5.1	13.8	6.65
		8.5	12.9	5.56			5.4	14.6	8.08
	ω	7.377	10.0	5.39		ω	4.599	7.12	3.54
		7.5	7.16	3.28			4.8	8.08	4.28
		8.0	8.58	2.16			5.1	12.6	2.59
		8.5	9.32	1.56			5.4	12.9	5.62
Ethane	C_p	4.872	12.6	6.07	Propane	C_p	4.248	12.3	6.36
		5.0	15.6	7.18			4.5	13.8	8.45
		5.3	16.3	9.08			4.8	14.6	7.29
		5.6	17.3	8.15			5.1	15.9	8.03
	κ_T	4.872	23.6	3.12		κ_T	4.248	20.4	1.54
		5.0	25.3	4.08			4.5	22.8	3.13
		5.3	29.4	6.18			4.8	25.9	5.21
		5.6	31.6	7.75			5.1	31.6	8.08
	α	4.872	25.9	3.08		α	4.248	22.8	4.86
		5.0	28.4	4.16			4.5	25.9	7.53
		5.3	30.6	6.27			4.8	27.5	8.16
		5.6	32.1	8.08			5.1	30.8	9.07
	μ	4.872	12.8	4.26		μ	4.248	10.1	.912
		5.0	14.6	4.16			4.5	11.6	1.54
		5.3	15.6	5.25			4.8	13.8	3.37
		5.6	18.8	6.84			5.1	15.4	5.29
	ω	4.872	8.05	2.37		ω	4.248	6.12	1.61
		5.0	8.43	2.48			4.5	7.08	1.95
		5.3	9.16	2.27			4.8	8.01	2.24
		5.6	9.98	2.30			5.1	8.94	2.37

$$AAD(\%) = (1/n)\cdot\left(\sum_i^n \left|(M_{i,exp} - M_{i,calc})/M_{i,exp}\right|\right)\times 100$$

$$\mu = T\left(\frac{\partial P}{\partial T}\right)_v - \rho\left(\frac{\partial P}{\partial \rho}\right)_T \quad (27)$$

$$C_p = C_v + \frac{T\alpha^2}{\kappa_T \rho} \quad (28)$$

$$\omega = \sqrt{\frac{C_p}{C_v}\left(\frac{\partial P}{\partial \rho}\right)_T} \quad (29)$$

Where C_v is the isochoric heat capacity, κ_T is the isothermal compressibility, α is the thermal expansivity, μ is the Joule-Thomson coefficient, C_p is the isobaric heat capacity, ω is the sound speed and A^{res} is the residual Helmholtz energy. The ideal gas heat capacity at constant volume C_v^{ideal} can be obtained from the following expression.

$$C_v^{ideal} = C_p^{ideal} - R \quad (30)$$

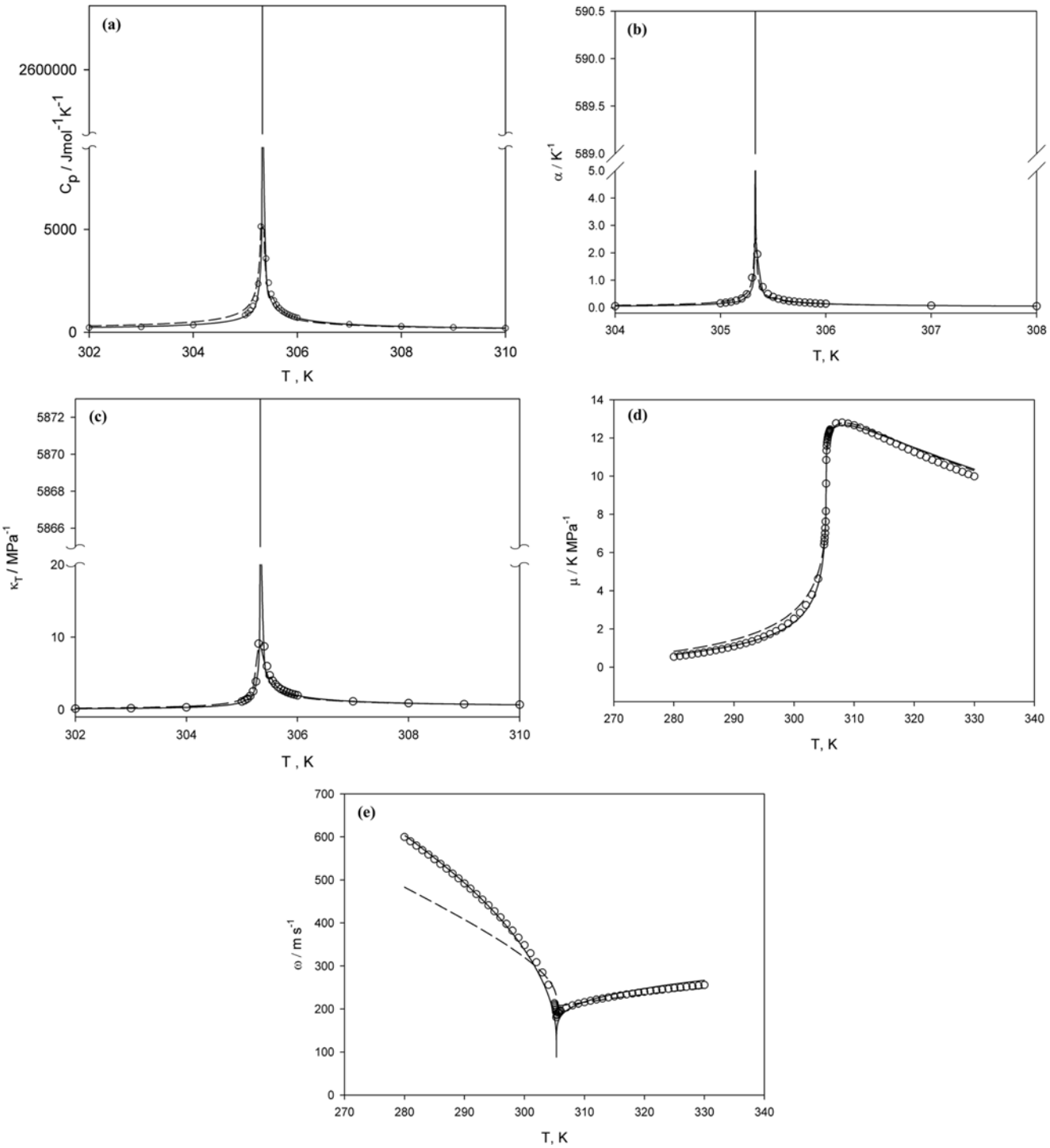

Fig. 3. Thermodynamic second order derivative properties of the QLF model (medium dashed curves) and the xQLF model (solid curves) for ethane. (a) isobaric heat capacity, (b) thermal expansion coefficient, (b) isothermal compressibility, (d) Joule-Thomson coefficient, (e) sound speed; ○, 4.872 MPa (=P_c).

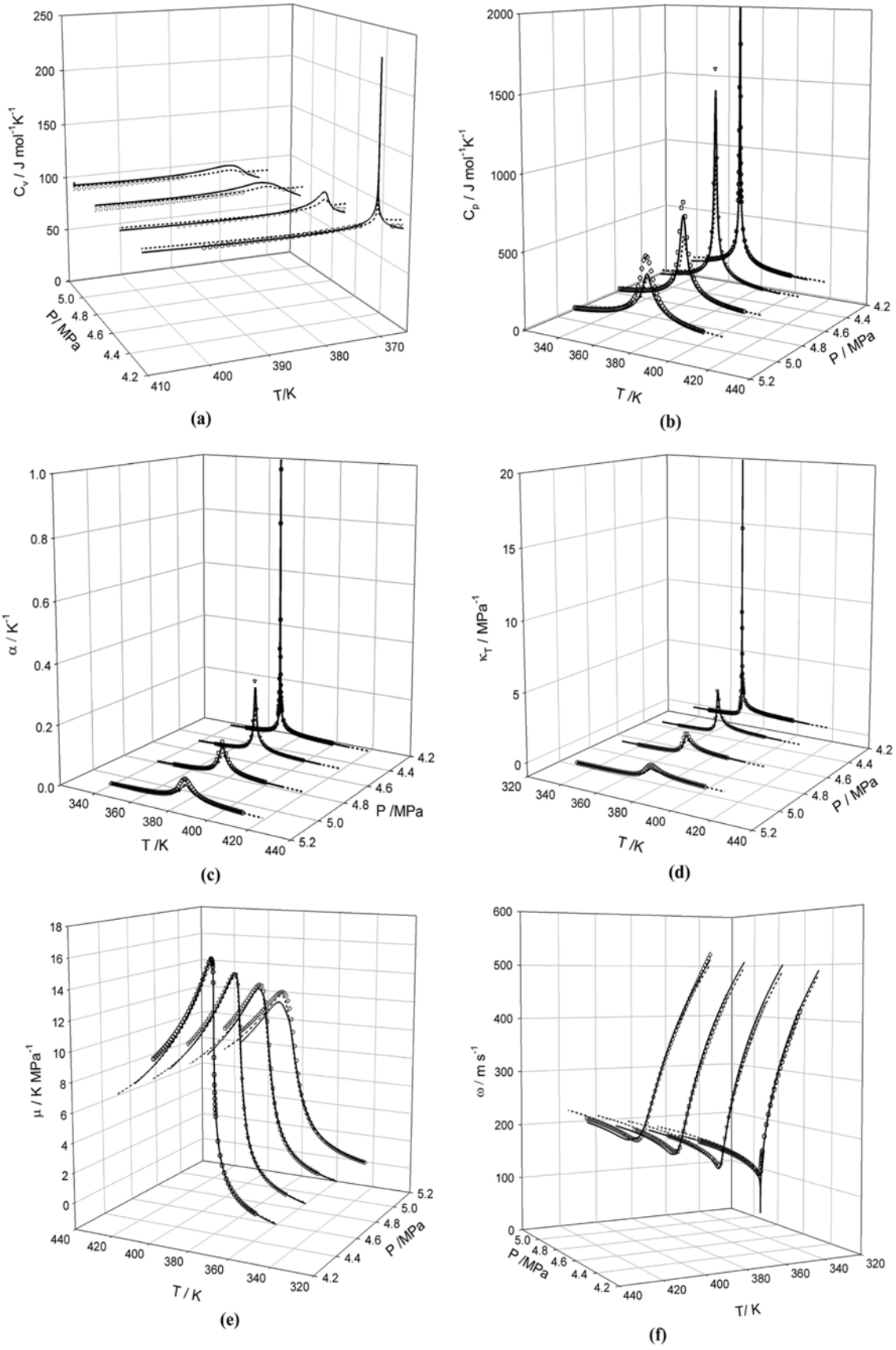

Fig. 4. Thermodynamic second order derivative properties of the crossover Patel-Teja model (short dashed curves) and the xQLF model (solid curves) for propane. (a) isochoric heat capacity, (b) isobaric heat capacity, (c) thermal expansion coefficient, (d) isothermal compressibility, (e) Joule-Thomson coefficient, (f) sound speed; ○, 4.248 MPa (=P_c); ▽, 4.5 MPa; □, 4.8 MPa; ◇, 5.1 MPa.

where C_p^{ideal} is the isobaric heat capacity of the ideal gas. For the correlation of the isobaric heat capacity of the ideal gas, the following equation is used:

$$C_p^{ideal}=A+BT+CT^2+DT^3+ET^4 \quad (31)$$

Coefficients (A, B, C, D) are taken from the NIST Chemistry WebBook [30].

RESULTS AND DISCUSSION

The xQLF model for pure fluids contains foursets of system-dependent parameters: (1) the classical parameters, T^*, P^* and ρ^*; (2) the crossover parameters, Gi, v_1 and d_1 (3) the critical shifts of fluids, $\Delta\tau_c$ and Δv_c, and (4) the Kernel term parameters, a_{20} and a_{21}. Since the real parameters T_c and v_c for pure fluids are usually known, $\Delta\tau_c$ and Δv_c are known too. Three sets ofparameters could be obtained by fitting the xQLF EOS to their experimental vapor pressure, saturated density and PρT data for pure fluids. All experimental data are obtained from the Korean thermophysical properties Databank (KDB) [31]. Six molecular parameters for pure fluids in the xQLF model are given in Table 1. We also find the last two kernel term parameters (a_{20}, a_{21}) by fitting the xQLF model to the experimental data [32-34] of isochoric heat capacity along the critical isochore. The kernelterm parameters for the xQLF model are listed in Table 2.

To test the accuracy of the xQLF model, it was compared with the classical QLF model, the crossover Sanchez-Lacombe (xLF) model [13] and the crossover cubic (xCubic) model [12]. The deviations of the VLE (vapor liquid equilibrium) and PρT properties calculated with the classical QLF, xQLF, xLF and xCubic model are listed in Tables 3 and 4. For all compounds, the xQLF model showed that the average absolute deviation (AAD) for vapor pressure is less than 0.77%, the AAD for saturated density is less than 0.69%, and the AAD for pressure of PρT properties is less than 1.25%. The xQLF model represented betteragreements with experimental data than the classical QLF model. Calculated result of the xQLF model, also, showed comparable to that of the xLF and the xCubic model. It is explained that the quasi-chemical approachof the xQLF model could be more important far from the critical point than near the critical region. In Figs. 1 and 2, the xQLF model prediction for VLE and PρT properties of carbon dioxide and n-hexane and is shown and compared with that from the classical QLF model and experimental data. From these figures, the classical QLF model apparently showed over-prediction of the critical pressure and critical temperature,while the xQLF model could achieve excellent agreement with experimental data both near and far from the critical region.

The deviation of the thermodynamic property data calculated with the QLF model and the xQLF model is listed Table 5. It shows that the average absolute deviation (AAD) for all properties is improved by the crossover approach. Fig. 3 depicts thermodynamic second order derivative properties of the QLF model and the xQLF model for ethane. Near the critical region, experimental data of C_p, κ_T, α show steep extremes, and those of ω, μ show drastic changes. The xQLF model shows an excellent agreement with experimental data which show singular behavior near the critical point. However, the classical QLF model does not describe the singular behavior. In the predictions of isobaric heat capacity, isothermal compressibility and thermal expansion coefficient, the QLF model showsthe maximum value at the critical point but does not predict singular behavior approaching infinity at the critical point. And the QLF model predicts the Joule-Thomson coefficient and sound speed with higher inaccuracies than those of the xQLF model. In Fig. 4, results for the comparison with estimations of the xQLF model and the crossover Patel-Teja model developed by Kiselev et al. [10] show that the xQLF model yields comparable to the crossover Patel-Teja model.

CONCLUSION

A crossover quasi-chemical nonrandom lattice fluid is presented. The quasi-chemical nonrandom lattice fluid model is combined with a crossover theory which incorporates the critical scaling laws valid asymptotically near the critical point and reduces to the original classical quasi-chemical nonrandom model far from the critical region. The crossover quasi-chemical nonrandom lattice fluid model reproduces volumetric properties and second-order derivative properties of fluids near to and far from the critical region. The quasi-chemical nonrandom lattice fluid model shows greater improvements than the classical quasi-chemical nonrandom model, and it yields comparable to the crossover Sanchez-Lacombe model and the crossover cubic model.

ACKNOWLEDGEMENT

This work was supported by Eulji University in 2010, a BK21 grant funded by the Ministry of Education, and by a National Research Foundation of Korea (NRF) grant funded by the Korean government (MEST) (No. NRF-2010-C1AAA001-2010-0028939).

NOMENCLATURE

a : Helmholtz free energy per mole
A : Helmholtz free energy
$\overline{A}$: dimensionless Helmholtz free energy
b^2 : universal linear-model parameter
d_1 : rectilinear diameter amplitude
Gi : Ginzburg number
P : pressure
R : gas constant
r : number of segments per molecule
T : temperature
V : volume
v : molar volume
v^* : close packed volume of a mer
z : lattice coordination number
Z : compressibility factor

Greek Letters

ε^* : molecular energy parameter
ρ : molar density
ρ^* : close packed molar density
φ : order parameter
$\overline{\varphi}$: renormalized order parameter
θ : surface area fraction
τ : reduced temperature difference
$\overline{\tau}$: renormalized temperature difference

Subscript

id : ideal gas state
r : residual properties

Superscript

0 : classical
c : critical
~ : reduced properties
* : characteristic properties

REFERENCES

1. J. M. H. Levelt-Sengers, *Fluid Phase Equilib.*, **158-160**, 3 (1999).
2. I. C. Sanchez and R. H. Lacombe, *J. Phys. Chem.*, **80**, 2352 (1976).
3. R. H. Lacombe and I. C. Sanchez, *J. Phys. Chem.*, **80**, 2368 (1976).
4. M. S. Shin and H. Kim, *Fluid Phase Equilib.*, **246**, 79 (2006).
5. M. S. Shin, K. P. Yoo, C. S. Lee and H. Kim, *Korean J. Chem. Eng.*, **23**, 469 (2006).
6. M. S. Shin, K. P. Yoo, C. S. Lee and H. Kim, *Korean J. Chem. Eng.*, **23**, 476 (2006).
7. K. Gauter and R. A. Heidemann, *Ind. Eng. Chem. Res.*, **39**, 1115 (2000).
8. H. C. Burstyn and J. V. Sengers, *Phys. Rev. Lett.*, **45**, 259 (1980).
9. J. V. Sengers and J. M. H. Levelt-Sengers, *Ann. Rev. Phys. Chem.*, **37**, 189 (1986).
10. S. B. Kiselev and D. G. Friend, *Fluid Phase Equilib.*, **162**, 51 (1999).
11. S. B. Kiselev and J. F. Ely, *Fluid Phase Equilib.*, **174**, 93 (2000).
12. Y. Lee, M. S. Shin, J. K. Yeo and H. Kim, *J. Chem. Thermodyn.*, **39**, 1257 (2007).
13. M. S. Shin, Y. Lee and H. Kim, *J. Chem. Thermodyn.*, **40**, 174 (2008).
14. Y. Lee, M. S. Shin, B. Ha and H. Kim, *J. Chem. Thermodyn.*, **40**, 741 (2008).
15. Y. Lee, M. S. Shin and H. Kim, *J. Chem. Phys.*, **129**, 203503 (2008).
16. S. S. You, K. P. Yoo and C. S. Lee, *Fluid Phase Equilib.*, **93**, 193 (1994).
17. S. S. You, K. P. Yoo and C. S. Lee, *Fluid Phase Equilib.*, **93**, 215 (1994).
18. M. S. Yeom, K. P. Yoo, B. H. Park and C. S. Lee, *Fluid Phase Equilib.*, **158-160**, 143 (1999).
19. J. W. Kang, J. H. Lee, K. P. Yoo and C. S. Lee, *Fluid Phase Equilib.*, **194-197**, 77 (2002).
20. M. S. Shin and H. Kim, *Fluid Phase Equilib.*, **256**, 27 (2007).
21. M. S. Shin and H. Kim, *J. Chem. Thermodyn.*, **40**, 1110 (2008).
22. S. Jang, M. S. Shin and H. Kim, *Korean J. Chem. Eng.*, **26**, 225 (2009).
23. M. S. Shin, J. H. Lee and H. Kim, *Fluid Phase Equilib.*, **272**, 42 (2008).
24. M. S. Shin and H. Kim, *Fluid Phase Equilib.*, **270**, 45 (2008).
25. C. I. Park, M. S. Shin and H. Kim, *J. Chem. Thermodyn.*, **41**, 30 (2009).
26. C. Panayiotou and J. H. Vera, *Polymer J.*, **14**, 681 (1982).
27. S. K. Kumar, U. W. Suter and R. C. Reid, *Ind. Eng. Chem. Res.*, **26**, 2532 (1987).
28. S. B. Kiselev and J. F. Ely, *Fluid Phase Equilib.*, **119**, 8645 (2003).
29. M. A. Anisimov, S. B. Kiselev, J. V. Sengers and S. Tang, *Physica A.*, **188**, 487 (1992).
30. E. W. Lemmon, M. O. McLinden and D. G. Friend, NIST Standard Reference Database Number 69, National Institute of Standards and Technology, Gaithersburg MD, 20899, http://webbook.nist.gov (2001).
31. J. Kang, K. Yoo, H. Kim, J. Lee, D. Yang and C. Lee, *Int. J. Thermophys.*, **22**, 487 (2001).
32. M. A. Anisimov, V. G. Beketov, V. P. Voronov, V. B. Nagaev and V. A. Smimov, *Teplofiz. Svoistva Veschestv Mater. (USSR)*, **16**, 124 (1982).
33. I. M. Abdulagatov, S. B. Kiselev, L. N. Levina, Z. R. Zakaryaev and O. N. Mamchonkova, *Int. J. Thermoyphys.*, **17**, 423 (1996).
34. I. M. Abdulagatov, N. G. Polikhronidi and R. G. Batyrova, *J. Chem. Thermodyn.*, **26**, 1031 (1994).